

## Activation and blockade of mouse muscle nicotinic channels by antibodies directed against the binding site of the acetylcholine receptor

J. Bufler, S. Kahlert, S. Tzartos\*, K. V. Toyka†, A. Maelicke‡ and Ch. Franke

*Neurologische Klinik der Technischen Universität München, Möhlstrasse 28,  
81675 München, Germany, \*Hellenic Pasteur Institute, 127 Vassilissis Sofias Avenue,  
Athens, 11521 Greece, †Neurologische Klinik der Universität Würzburg,  
Josef-Schneiderstrasse 12, 97080 Würzburg and ‡Institut für Physiologische Chemie  
und Pathobiochemie der Universität Mainz, Duesbergweg 6, 55128 Mainz, Germany*

1. Using the patch-clamp technique, we have found that mouse muscle nicotinic acetylcholine receptor (nAChR) channels can be activated by low concentrations of a monoclonal antibody (MoAb), referred to as WF6, which is directed against the acetylcholine (ACh) binding site. Similar effects were seen using IgG or F(ab)<sub>2</sub> fragments from the sera of patients with myasthenia gravis (MG), which contain polyclonal anti-nAChR antibodies.
2. The mean open times of MoAb and the slope conductance of single WF6-activated single channels were similar to those of ACh-activated channels under the same experimental conditions.
3. On outside-out patches, single channel activity was elicited by MoAb WF6 and MG F(ab)<sub>2</sub> fragments, and was blocked by (+)-tubocurarine. We therefore concluded that MoAb WF6 and the MG F(ab)<sub>2</sub> fragments activate the nAChR.
4. MoAb WF6 and MG F(ab)<sub>2</sub> fragments blocked the current activated by pulsed application of 10<sup>-4</sup> M ACh to a significant extent. The block was partly reversible. The rate constants for the binding and dissociation of MoAb WF6 from the receptor were determined quantitatively.

Myasthenia gravis (MG) is caused by the chronic attack of muscle endplates by anti-nicotinic acetylcholine receptor (anti-nAChR) antibodies, which results in a loss of functional nAChRs. Three mechanisms are implicated: (1) increased rate of nAChR degradation; (2) complement-mediated destruction of postsynaptic membranes; and (3) direct block of nAChR function (for examples see Goldberg, Mochly-Rosen, Fuchs & Lass, 1983; Maselli, Nelson & Richman, 1989; Burgess, Wray, Pizzighella, Hall & Vincent, 1990). The main electrophysiological abnormalities can be transferred passively from man to mouse by injection of MG IgG (Toyka, Drachmann, Pestronk & Kao, 1975). In this study we have used the patch-clamp technique to investigate, on the molecular level, the acute electrophysiological effects of antibodies directed against different epitopes of the nAChR.

### METHODS

Patch-clamp recordings, obtained from cultured embryonic mouse myotubes (mice were killed by cervical dislocation, see Franke, Költgen, Hatt & Dudel, 1992) whose nAChR is made up of  $\alpha_2\beta\gamma\delta$ -

subunits (embryonic type) were made in the cell-attached and in the outside-out configuration, using standard protocols (Hamill, Marty, Neher, Sakmann & Sigworth, 1981). For experiments in the cell-attached mode, the respective antibody was added in the indicated concentrations to the patch pipette containing the extracellular solution. The liquid filament switch technique (Franke, Hatt & Dudel, 1987) was used for pulsed application of antibodies to outside-out patches. Using this method, solution exchange is completed within 200–300  $\mu$ s. In total, twenty-five cell-attached patches and sixty-four outside-out patches were analysed.

Single channel currents were recorded with a List EPC7 patch-clamp amplifier for cell-attached recordings or a List EPC9 patch-clamp amplifier for outside-out patch recordings. The data were stored on a modified Sony DAT-recorder, and they were low-pass filtered at 1 kHz for measurements with the cell-attached configuration and at 2 kHz for measurements with the outside-out configuration. For off-line evaluation of single channel data, an event-detection program was used for the construction of open and closed time histograms (Dudel & Franke, 1987).

The composition of the extracellular solution was (mM): 137 NaCl, 5.3 KCl, 0.67 Na<sub>2</sub>HPO<sub>4</sub>, 0.22 KH<sub>2</sub>PO<sub>4</sub>, 15 Hepes, 5.6 glucose, 1 CaCl<sub>2</sub>. The pH was adjusted to 7.3 with 1 M NaOH and the

osmolarity to 315 mosmol l<sup>-1</sup> with mannitol. The intracellular solution was composed of (mM):140 KCl, 11 EGTA, 10 Hepes, 10 glucose, 2 MgCl<sub>2</sub>. The pH was adjusted to 7.3 with 1 M KOH and the osmolarity to 315 mosmol l<sup>-1</sup> with mannitol.

In cell-attached measurements, the membrane potential is the sum of the actual pipette potential plus the resting potential of the myotube. The resting potential varied between -40 and -60 mV and was not determined for each experiment.

The liquid filament switch technique (Franke *et al.* 1987) was used for pulsed application of antibodies to outside-out patches. It was not possible to include the respective purified antibody preparations in the background solution of the system for the liquid filament switch, due to insufficient material for a long-term incubation of a patch at a flow rate of background solution of 1 ml min<sup>-1</sup>. The following pulse protocol was therefore used: six successive pulses of 10<sup>-4</sup> M ACh of 400 ms duration with an interval of 5 s between pulses (allowing complete recovery from desensitization) were applied to the patch. Subsequently, one 60 s pulse of the respective antibody-containing solution was applied. This pulse alternated with six short pulses of 10<sup>-4</sup> M ACh plus antibodies; this cycle was repeated as required (the arrows on the time axis of Fig. 4B and E indicate the point of time of the test pulses). When the peak current amplitude had stabilized at a low value due to the block, the test solution was changed to a solution without antibodies. Again, six test pulses were applied at different time intervals to determine the recovery from the block. To calculate the binding constant, the time constant of block of the respective antibody preparation was calculated by fitting the time course of block with a single exponential (Fig. 4B and E, dashed line) by least squares. To calculate the dissociation rate of the monoclonal antibody (MoAb) WF6, we used the time from the beginning of the recovery to 50% of the steady-state value, not assuming complete recovery from the block.

All experimental data were given as means ± s.e.m.

The antibodies used were prepared as described elsewhere. For MoAb WF6 see Fels, Plümer-Wilk, Schreiber & Maelicke (1986) and Conti-Tronconi, Tang, Diethelm, Spencer, Reinhardt-Maelicke & Maelicke (1990). There is only one WF6 binding site per nAChR monomer, i.e. one half as many as ACh binding sites (Fels *et al.* 1986). For IgG and F(ab)<sub>2</sub> fragments from myasthenic patients (experiments were performed with IgG and with F(ab)<sub>2</sub> fragments from two different myasthenic patients) see Sterz *et al.* (1986) and Toyka *et al.* (1980). The human F(ab)<sub>2</sub> fragments were tested using human muscle nAChR; reaction with mouse nAChR is normally 1:1 to 1:100 less (Garlepp, Kay, Dawkins, Bucknall & Kemp, 1981). For MoAb 35, an antibody directed against the main immunogenic region of the nAChR (amino acid (AA) sequence, α6-85) see Tzartos, Kokla, Walgrave & Conti-Tronconi (1988) and for MoAb 155, an antibody directed against a cytoplasmic region of the nAChR α-subunit (AA α373-380) see Tzartos & Remoundos (1992). MoAb 35 and MoAb 155 were assayed by double precipitation using mouse nAChR. Further control experiments were performed with WF20, an antibody binding distant from the ACh and WF6 binding site on the α-subunit (Watters & Maelicke, 1983). The exact binding site of this MoAb is not known, however. Another control was done with normal human IgG (Venimmun®, a commercially available polyvalent human 7-S IgG preparation; Behring, Mannheim, Germany).

Antibody titres were assayed by a double immunoprecipitation assay modified from Lindstrom (Toyka *et al.* 1980; Sterz *et al.* 1986). The molarity of MoAb WF6 and WF20 was determined as described in Fels *et al.* (1986) and Watters & Maelicke (1983), of MoAb 35 and MoAb 155 as described in Tzartos *et al.* (1988) and Tzartos and Remoundos (1992), and of MG IgG and MG F(ab)<sub>2</sub> fragments as described in Sterz *et al.* (1986). All antibody preparations were dialysed and sterile filtered using Millipore filters, pore size 0.22 μm.

## RESULTS

To investigate the effect of MoAb WF6, the major epitope of which is located within the α-subunit AA sequence α181-200 (Conti-Tronconi *et al.* 1990 and Schröder *et al.* 1994) of *Torpedo marmorata* nAChR, it was added to the physiological solution in the patch pipette and we recorded in the cell-attached configuration. Under these conditions, single channel activity was observed regularly (Fig. 1B). Similar single channel activity was recorded in the cell-attached mode after MG IgG fractions (Fig. 1C) were added to the solution in the patch pipette. The configuration of the antibody-activated single channels seems to be very similar to that of ACh-activated channels (10<sup>-6</sup> M, Fig. 1A).

In Fig. 1, beside the original registrations, evaluations of mean open time of single channel openings are shown for the respective test solution. The open time distributions were fitted with a single exponential. Twelve experiments were evaluated; the mean open time was 1.40 ± 0.39 ms (ACh, *n* = 4); 1.51 ± 0.26 ms (MoAb WF6, *n* = 5); and 1.47 ± 0.28 ms (MG IgG, *n* = 3).

In addition, the single channel current amplitude was analysed at different membrane potentials. In Fig. 2A, the single channel current amplitude is plotted at different potentials (given as the actual pipette potential). The linear fit of nine such experiments resulted in a slope conductance of 47.0 ± 1.4 pS (*n* = 3), 45.7 ± 1.1 pS (*n* = 3) and 44.7 ± 0.9 pS (*n* = 3) for ACh-, MoAb WF6- and MG IgG-activated single channels, respectively (Fig. 2A). Each experiment had to be evaluated individually, since the resting potential of the cells varied; note the parallel shift of the curves in Fig. 2A (see Methods).

We noted that the frequency of single channel openings elicited by MoAb WF6 decreased substantially during the measurements. In the case of Fig. 2B, it decreased from around 55 to 15 openings s<sup>-1</sup> during the first 120 s of registration. This indicates a slow desensitization of the WF6-activated single channels, as previously described for ACh-activated single nicotinic channels (Ochoa, Chattopadhyay & McNamee, 1989).

A control MoAb, WF20 (7 × 10<sup>-8</sup> M, anti-nAChR antibody directed against a site distant from the ACh binding site) did not elicit single channel openings (*n* = 5, data not shown).

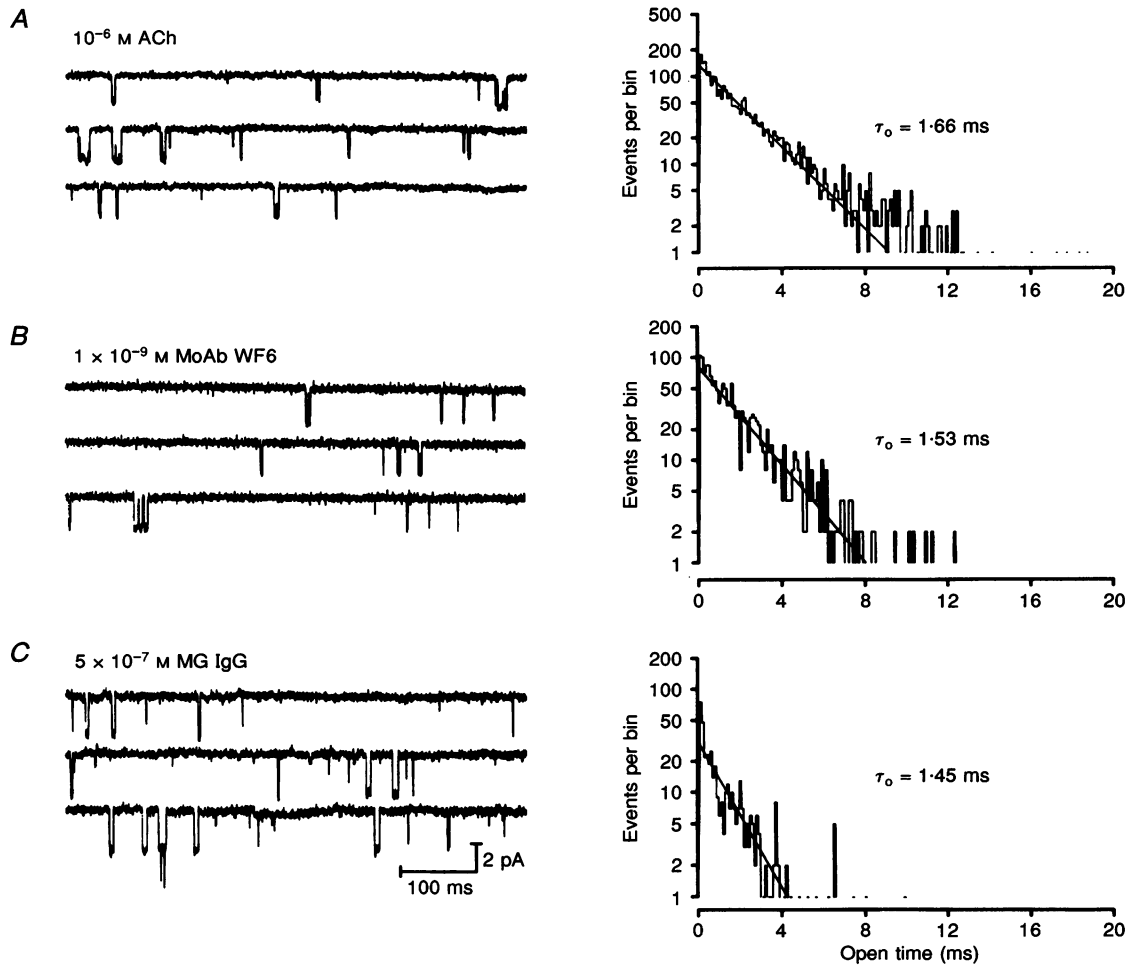


**Figure 1.** Single channel recordings from embryonic mouse muscle using the patch-clamp technique in the cell-attached configuration

*A*, single channels activated by  $10^{-6}$  M ACh. *B*, single channels activated by  $1 \times 10^{-9}$  M MoAb WF6. *C*, single channels activated by  $5 \times 10^{-7}$  M MG IgG fractions. The respective histograms of open times are shown on the right. Pipette potential for all measurements was  $-10$  mV.  $\tau_o$ , mean open time.

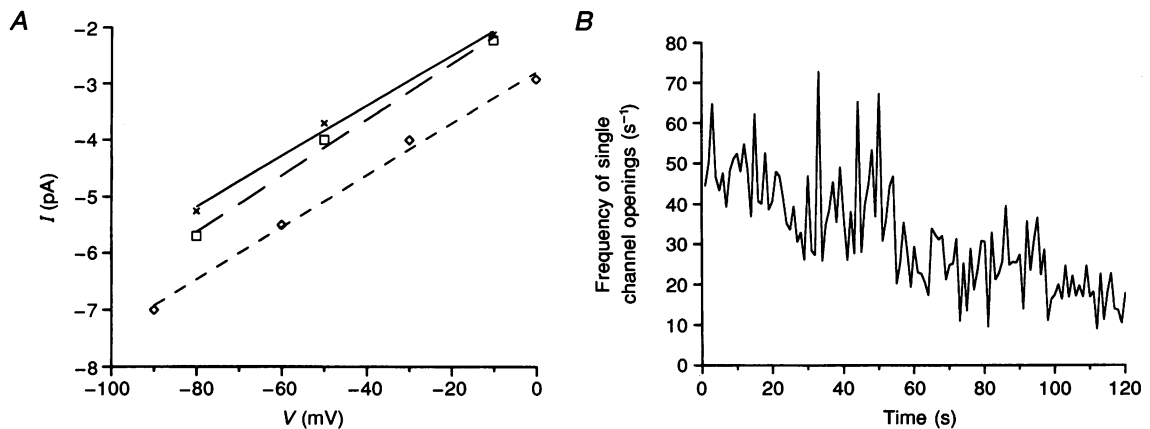


**Figure 2**

*A*, dependence of the single channel current amplitude on pipette potential (continuous line, MoAb WF6; long dashed line, ACh; short dashed line, MG IgG). *B*, time dependence of the frequency of single channel openings activated by  $1 \times 10^{-9}$  M WF6. The frequency of single channel openings each second was measured for 120 s. Second 1 in the figure was approximately 10 s after formation of the gigaohm seal.

Single channel activity was also elicited by the MoAb WF6 if it was applied to outside-out patches with the fast application system. Figure 3A shows single channel openings during a 5 s pulse containing  $7 \times 10^{-9}$  M WF6. In the 10 s interval between pulses, single channel activity was not observed. If  $1 \times 10^{-5}$  M (+)-tubocurarine was added to the MoAb WF6-containing test solution and to the background solution of the fast application system, single channel openings could not be observed (Fig. 3B), indicating block of MoAb WF6-activated single channels by (+)-tubocurarine.

The same effect was observed using purified F(ab)<sub>2</sub> fragments of the IgG fraction of a MG patient (Toyka *et al.* 1980; Sterz *et al.* 1986). Pulsed application of F(ab)<sub>2</sub>

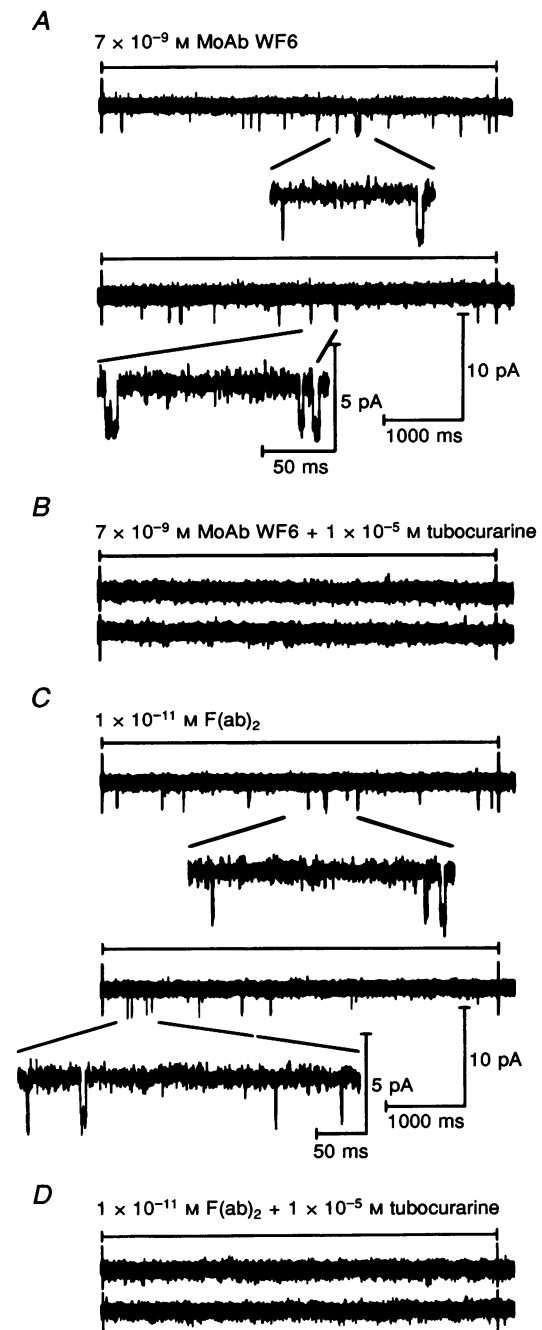
fragments elicited single channel openings (Fig. 3C), which were blocked by  $1 \times 10^{-5}$  M (+)-tubocurarine added to the test solution (Fig. 3D). Additionally, the single channel activity elicited by F(ab)<sub>2</sub> fragments or MoAb WF6 could not be observed if  $10^{-4}$  M ACh was added to the test solution, suggesting desensitization of nicotinic receptors by ACh ( $n = 5$ , not shown).

So far we concluded that the MoAb WF6, MG IgG fractions and MG F(ab)<sub>2</sub> fragments activated nicotinic channels (Figs 1A–C, 2A and 3A–D).

In the next series of experiments, we applied pulses of ACh to outside-out patches. With experiments of this type, all rate constants which are necessary to describe activation and desensitization of the nAChR could be determined

### Figure 3. Activation of single channels by pulsed application of antibodies

*A*, activation of single channels by pulsed application (pulse duration 5 s) of  $7 \times 10^{-9}$  M MoAb WF6. *B*, block of the single channels after addition of  $1 \times 10^{-5}$  M (+)-tubocurarine to the MoAb WF6-containing test solution (pulse duration, 5 s). *C*, activation of single channels by pulsed application (pulse duration, 5 s) of  $1 \times 10^{-11}$  M MG F(ab)<sub>2</sub> fragments. *D*, block of the single channels after addition of  $1 \times 10^{-5}$  M (+)-tubocurarine to the MG F(ab)<sub>2</sub> fragments containing test solution (pulse duration, 5 s). In panels *A* and *C*, some single channel events are shown on a different time scale. Holding potential for all measurements was  $-60$  mV.



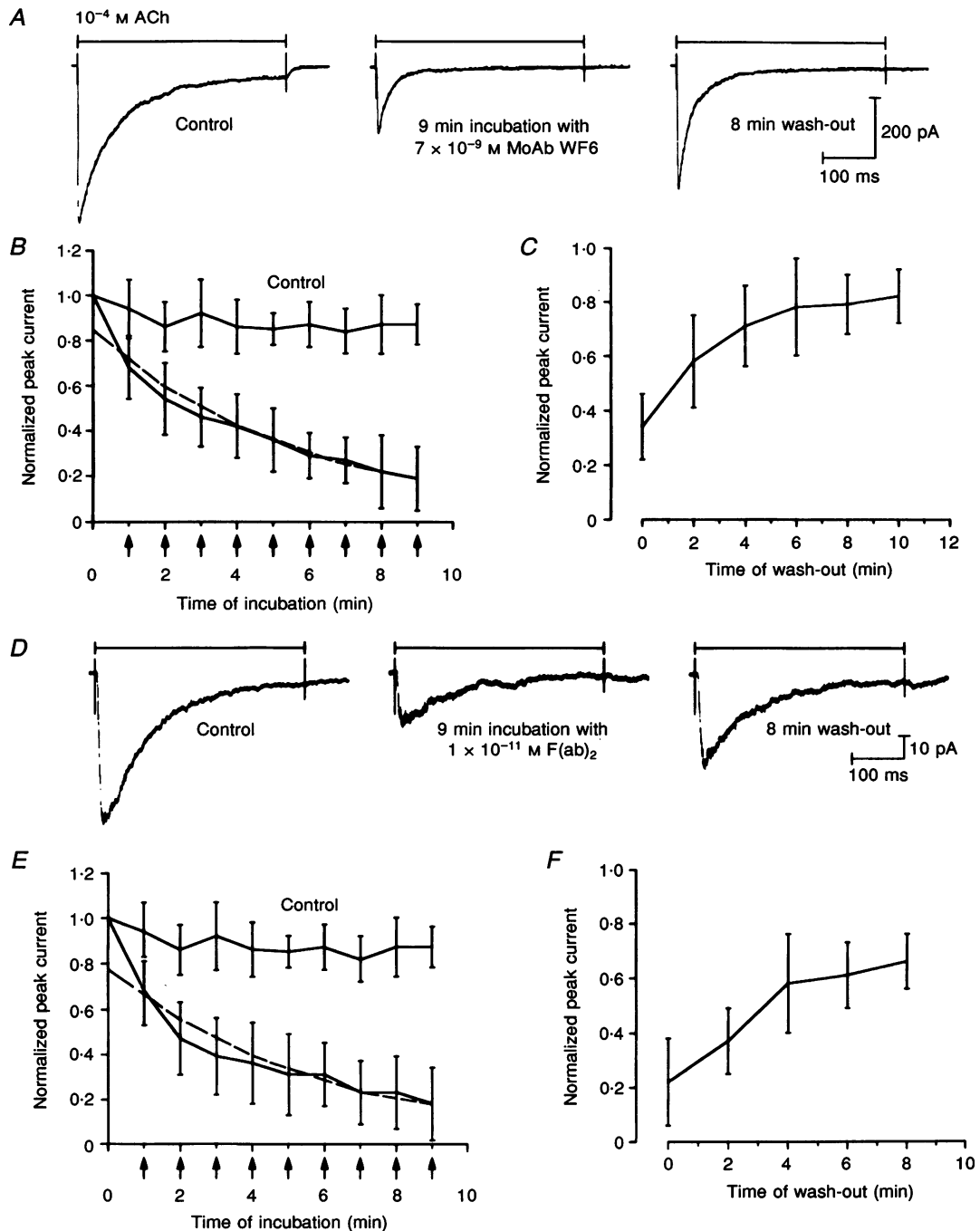


**Figure 4.** Investigation of the acute blocking effect of anti-nAChR antibodies

Recordings of nAChR-activated channels on outside-out patches using the liquid filament switch technique. *A*, fast activation of nAChRs (averaged current of 6 single activations) by 400 ms pulses of a test solution containing  $10^{-4}$  M ACh in the beginning of the experiment, after 9 min of incubation with  $7 \times 10^{-9}$  M MoAb WF6 (middle trace) and following 8 min of wash-out. *B*, plot of the time dependence of the peak current amplitude relative to the control (lower line,  $n = 15$ ; dashed line, single exponential fit of the time course of block). The upper line shows control experiments in the absence of MoAb WF6 ( $n = 9$ ). Here and in *E*, arrows indicate point of time of the 6 pulses of  $10^{-4}$  M ACh, applied every 60 s. *C*, plot of the peak current amplitude elicited by  $10^{-4}$  M ACh during wash-out of MoAb WF6;  $n = 4$ . *D*, fast activation of nAChRs (averaged current of 6 single activations) by 400 ms pulses of a test solution containing  $10^{-4}$  M ACh in the beginning of the experiment, after 9 min of incubation with  $1 \times 10^{-11}$  M F(ab)<sub>2</sub> fragments (middle trace) and following 8 min of wash-out. *E*, plot of the time dependence of the peak current amplitude relative to the control (lower line,  $n = 19$ ; dashed line, single exponential fit of the time course of block). The upper line shows control experiments in the absence of F(ab)<sub>2</sub> fragments ( $n = 9$ ). *F*, plot of the peak current amplitude elicited by  $10^{-4}$  M ACh during wash-out of the F(ab)<sub>2</sub> fragments ( $n = 12$ ). Bars show the s.e.m.

Table 1. Blocking effects of different antibody preparations

	Binding site at nAChR $\alpha$ -subunit	Protein concentration (M)	$\alpha$ -Bungarotoxin binding sites (M)	Incubation time (min)	Relative current amplitude
MoAb WF6	AA $\alpha$ 181–200	$7 \times 10^{-9}$	—	9	$0.19 \pm 0.14$ (15)
F(ab) <sub>2</sub> fragments	—	$1 \times 10^{-11}$	$0.75 \times 10^{-12}$	9	$0.18 \pm 0.16$ (18)
MoAb WF20	Distant from binding site	$7 \times 10^{-8}$	—	11	$0.89 \pm 0.10$ (5)
MoAb 35	AA $\alpha$ 6–85	$7 \times 10^{-9}$	$3 \times 10^{-9}$	8	$0.91 \pm 0.11$ (7)
MoAb 155	AA $\alpha$ 373–380	$1 \times 10^{-8}$	$3 \times 10^{-9}$	9	$0.98 \pm 0.05$ (6)
Normal human IgG	—	$1 \times 10^{-5}$	$< 0.1 \times 10^{-9}$	8	$0.96 \pm 0.05$ (3)

The percentage of block was compared with the normalized peak amplitude of the current elicited by  $10^{-4}$  M ACh at the beginning of the respective experiment (Fig. 4A and D). Protein and  $\alpha$ -bungarotoxin binding site concentrations are as calculated for the final dilutions used in the experiments. Values are given as means  $\pm$  s.e.m. Numbers in parentheses indicate the number of experiments.

quantitatively (Franke, Hovav, Parnas & Dudel, 1993). After the beginning of a pulse with a saturating concentration of  $10^{-4}$  M ACh, the current amplitude increases within 1 ms to a peak value and decays to a low steady-state value due to desensitization (see first traces in Fig. 4A and D, see also Franke *et al.* 1993). We then added different antibody preparations to the test solution to investigate the blocking effect of the MoAb WF6 and of MG F(ab)<sub>2</sub> fragments; 75% of the tests with MoAb WF6 and 90% of the tests with the MG F(ab)<sub>2</sub> fragments showed a reduction in peak current of  $> 30\%$ .

The first trace in Fig. 4A shows the current elicited by pulsed application of  $10^{-4}$  M ACh. After 9 min incubation of the outside-out patch with  $7 \times 10^{-9}$  M of MoAb WF6, the peak amplitude of the current elicited by  $10^{-4}$  M ACh was reduced (middle trace of Fig. 4A). The block was partly reversed after 8 min wash-out (third trace of Fig. 4A). Additionally, control experiments were done in which  $10^{-4}$  M ACh was applied without any antibody. In Fig. 4B, the results of control experiments and of experiments with the MoAb WF6 are shown. The normalized peak current decreased after 9 min incubation with the MoAb to  $0.19 \pm 0.14$  ( $n = 15$ ). In the controls, the current decreased only slightly to  $0.87 \pm 0.09$  ( $n = 9$ ), due to a non-specific run-down of channels. The time course of the block by MoAb WF6 was fitted with a single exponential (Fig. 4B, dashed line) with a time constant of  $355 \pm 95$  s ( $n = 15$ ). Assuming that this time constant reflects the binding of MoAb WF6 to the nAChR, the rate constant was  $0.4 \times 10^6 \pm 0.06 \times 10^6$  M<sup>-1</sup> s<sup>-1</sup> ( $n = 15$ ), similar to the value determined by direct association kinetics with <sup>3</sup>H-labelled WF6 (Fels *et al.* 1986).

Figure 4C shows the increase of the amplitude of the normalized peak current elicited by  $10^{-4}$  M ACh during the wash-out of the MoAb. After 10 min of wash-out, the normalized peak current was  $0.82 \pm 0.12$  ( $n = 4$ ). The rate constant of dissociation of MoAb WF6 was (using the 50%

recovery time, see Fig. 4C)  $8.5 \times 10^{-3} \pm 1.9 \times 10^{-3}$  s<sup>-1</sup> ( $n = 4$ ), about four orders of magnitude larger than that determined for complexes with *Torpedo* receptor (Fels *et al.* 1986), and the equilibrium dissociation constant ( $K_D$ ) was determined to be  $28 \times 10^{-9} \pm 8.5 \times 10^{-9}$  M (three orders of magnitude larger than for the *Torpedo* receptor).

Figure 4D–F shows the results of experiments using purified F(ab)<sub>2</sub> fragments from a MG patient, together with control experiments. The normalized peak current amplitude was  $0.18 \pm 0.16$  ( $n = 19$ ) after 9 min of incubation with  $1 \times 10^{-11}$  M MG F(ab)<sub>2</sub> fragments (Fig. 4E). The time course of the block was fitted with a single exponential, with a time constant of  $365 \pm 155$  s ( $n = 19$ ). After an 8 min wash-out time the peak current amplitude was  $0.66 \pm 0.11$  ( $n = 13$ , Fig. 4F). Because only an unknown fraction of the MG F(ab)<sub>2</sub> fragments will be effective, the rate constants of binding and unbinding of F(ab)<sub>2</sub> fragments were not calculated.

To determine whether blockade was only produced by antibodies directed against the ACh binding site, further experiments were performed using polyclonal normal human IgG and MoAb, not directed against the nAChR binding site (see Table 1). No blocking effect exceeding the run-down phenomenon of the ACh-activated current was observed during an incubation time of 8 min (normal human IgG,  $n = 3$ ), 11 min (MoAb WF20,  $n = 5$ ), 8 min (MoAb 35,  $n = 7$ ) and 9 min (MoAb 155,  $n = 6$ ) with any of these antibodies (Table 1).

## DISCUSSION

For all of the MoAbs used in this study, their epitopes on the  $\alpha$ -subunit of the respective nAChR have been determined at the peptide level (Table 1).

The MoAb directed against the ACh binding site of *Torpedo* receptor (WF6, Figs 1B and 3A), MG IgG fractions (Fig. 1C) and MG F(ab)<sub>2</sub> fragments (Fig. 3C) caused single

channel activation, with single channel kinetics similar to those of ACh-activated single channels (Fig. 1A) under the same experimental conditions and to those previously reported by others for frog nicotinic receptors (Colquhoun & Sakmann, 1985), which have kinetic properties very similar to those of mouse nicotinic receptors. In contrast, the MoAb WF20, binding not at the binding site of the receptor, did not induce single channel openings. In addition, the single channel activity elicited by MoAb WF6 and MG F(ab)<sub>2</sub> fragments was blocked by (+)-tubocurarine (see Fig. 3B and D) and desensitizing concentrations of ACh. We therefore concluded that the MoAb directed against the binding site (WF6) and MG IgG fractions or MG F(ab)<sub>2</sub> fragments activated the nicotinic receptor.

The activation of nicotinic channels by MoAb WF6 was tested at low concentrations ( $1 \times 10^{-9}$  M or  $7 \times 10^{-9}$  M, see Figs 1B and 3A). Because the binding and dissociation rates of MoAb WF6 to the nicotinic receptor are very low compared to those of ACh (Franke *et al.* 1993), it is not expected that 'macroscopic' currents with fast activation and desensitization kinetics could be mimicked by MoAb WF6.

Out of four MoAbs (MoAb WF6, MoAb WF20, MoAb 155, MoAb 35, see Table 1), only MoAb WF6, binding to the binding site of the receptor, led to a reversible blockade of the nAChRs. There is a discrepancy between our results showing a reversible (low affinity) block of the nAChR by MoAb WF6 and those obtained with binding studies (Fels *et al.* 1986). As shown previously for  $\alpha$ -neurotoxins (Maelicke, Fulpius, Klett & Reich, 1977; Kang & Maelicke, 1980), it may be that binding proceeds in several stages, with the first stage being of relatively low affinity resulting in reversible block due to a four orders of magnitude larger unbinding rate as measured in our experiments (Fig. 4C). With binding studies it was shown that there is only one MoAb WF6 binding site per receptor monomer (Fels *et al.* 1986). It remains unclear, however, how many MoAbs bind to one nAChR with low affinity, producing the reversible block and probably also single channel activation.

Polyvalent MG IgG fractions or MG F(ab)<sub>2</sub> fragments would be expected to bind to multiple sites on the nAChR, including the main immunogenic region and the ACh binding site of the  $\alpha$ -subunit. Although we found only MoAb WF6, directed against the binding site, affecting the function of the nAChR (see Table 1), it is not proven that block of the nAChR is caused exclusively by antibodies directed against the binding site. Because in most cases of MG, polyvalent antibodies directed against the nAChR are detected, it is probable that there are other epitopes on the receptor, additional to the binding site, which affect the function of nAChRs. However, antibodies binding at or near the binding site are not, or only marginally, detected by the diagnostic double immunoprecipitation assay (Vincent *et al.* 1993). Therefore, in analogy with the WF6 results, it

may be that mainly antibody binding to the ACh binding site of the  $\alpha$ -subunit is responsible for the fast electrophysiological effects of activation and block of the receptor.

Our observations may help to understand some hitherto unexplained pathophysiological features of the autoimmune disorder MG, such as the rapid fluctuations of muscle weakness and the very rapid recovery of muscle strength after therapeutic plasmapheresis, which occurs faster than the turnover of nAChRs at the neuromuscular endplate.

- BURGESS, J., WRAY, D. W., PIZZIGHELLA, S., HALL, Z. & VINCENT, A. (1990). A myasthenia gravis plasma immunoglobulin reduces miniature endplate potentials at human endplate *in vitro*. *Muscle and Nerve* **13**, 407–413.
- COLQUHOUN, D. & SAKMANN, B. (1985). Fast events in single-channel currents activated by acetylcholine and its analogues at the frog muscle endplate. *Journal of Physiology* **369**, 501–557.
- CONTI-TRONCONI, B. M., TANG, F., DIETHELM, B. M., SPENCER, R., REINHARDT-MAELICKE, S. & MAELICKE, A. (1990). Mapping of a cholinergic binding site by means of synthetic peptides, monoclonal antibodies, and  $\alpha$ -bungarotoxin. *Biochemistry* **29**, 6221–6230.
- DUDEL, J. & FRANKE, C. (1987). Single glutamate-activated synaptic channels at the crayfish neuromuscular junction: II Dependence of channel open time on glutamate concentration. *Pflügers Archiv* **408**, 307–314.
- FELS, G., PLÜMER-WILK, R., SCHREIBER M. & MAELICKE, A. (1986). A monoclonal antibody interfering with binding and response of the acetylcholine receptor. *Journal of Biological Chemistry* **261**, 15746–15754.
- FRANKE, C., HATT, H. & DUDEL, J. (1987). Liquid filament switch for ultra-fast exchanges of solutions at excised patches of synaptic membrane of crayfish muscle. *Neuroscience Letters* **77**, 199–204.
- FRANKE, C., HOVAV, G., PARNAS, H. & DUDEL, J. (1993). A molecular scheme for the interaction between agonist and nicotinic receptor. *Biophysical Journal* **64**, 339–356.
- FRANKE, CH., KÖLTGEN, D., HATT, H. & DUDEL, J. (1992). Activation and desensitization of embryonic-like receptor channels in mouse muscle by acetylcholine concentration steps. *Journal of Physiology* **451**, 145–158.
- GARLEPP, M. J. H., KAY, P. H., DAWKINS, R. L., BUCKNALL, R. C. & KEMP, A. (1981). Cross reactivity of anti-acetylcholine receptor autoantibodies. *Muscle and Nerve* **4**, 282–288.
- GOLDBERG, G., MOCHLY-ROSEN, D., FUCHS, S. & LASS, Y. (1983). Monoclonal antibodies modify acetylcholine induced ionic channel properties in cultured chick myoballs. *Journal of Membrane Biology* **76**, 123–128.
- HAMILL, O. P., MARTY, A., NEHER, E., SAKMANN, B. & SIGWORTH, F. J. (1981). Improved patch-clamp techniques for high resolution current recordings from cells and cell-free patches. *Pflügers Archiv* **391**, 85–100.
- KANG, S. & MAELICKE, A. (1980). FITC-labeled  $\alpha$ -cobratoxin; biochemical characterization and interaction with acetylcholine receptor from *Electrophorus electricus*. *Journal of Biological Chemistry* **255**, 7326–7332.
- MAELICKE, A., FULPIUS, B. W., KLETT, R. P. & REICH, E. (1977). Acetylcholine receptor. Responses to drug binding. *Journal of Biological Chemistry* **252**, 4811–4830.

- MASELLI, R. A., NELSON, D. J. & RICHMAN, D. P. (1989). Effects of a monoclonal anti-acetylcholine receptor antibody on the avian endplate. *Journal of Physiology* **411**, 271–283.
- OCHOA, E. L. M., CHATTOPADHYAY, A. & MCNAMEE, M. G. (1989). Desensitization of the nicotinic acetylcholine receptor: Molecular mechanisms and effect of modulator. *Cellular and Molecular Neurobiology* **9**, 141–178.
- SCHRÖDER, B., REINHARDT, S., SCHRATTENHOLZ, A., MCLANE, K., KRETSCHNER, A., CONTI-TRONCONI, B. M. & MAELICKE, A. (1994). Monoclonal antibodies FK1 and WF6 define two neighboring ligand binding sites on *Torpedo* acetylcholine receptor  $\alpha$ -polypeptide. *Journal of Biological Chemistry* **269**, 10407–10416.
- STERZ, R., HOHLFELD, R., RAJKI, K., KAUL, M., HEININGER, K., PEPPER, K. & TOYKA, K. V. (1986). Effector mechanisms in myasthenia gravis: endplate function after passive transfer of IgG, Fab and F(ab')<sub>2</sub> hybrid molecules. *Muscle and Nerve* **9**, 305–312.
- TOYKA, K. V., DRACHMANN, D. B., PESTRONK, A. & KAO, I. (1975). Myasthenia gravis: passive transfer from man to mouse. *Science* **190**, 397–399.
- TOYKA, K. V., LÖWENADLER, B., HEININGER, K., BESINGER, U. A., BIRNBERGER, K. L., FATEH-MOGHADAM, A. & HEILBRONN, E. J. (1980). Passively transferred myasthenia gravis: protection of mouse endplates by Fab fragment from human myasthenic IgG. *Journal of Neurology, Neurosurgery and Psychiatry* **48**, 836–842.
- TZARTOS, S. J., KOKLA, A., WALGRAVE, S. L. & CONTI-TRONCONI, B. M. (1988). Localization of the main immunogenic region of human muscle acetylcholine receptor to residues 67–76 of the  $\alpha$ -subunit. *Proceedings of the National Academy of Sciences of the USA* **85**, 2899–2903.
- TZARTOS, S. J. & REMOUNDOS, M. (1992). Precise epitope mapping of monoclonal antibodies to the cytoplasmic side of the acetylcholine receptor  $\alpha$ -subunit. *European Journal of Biochemistry* **207**, 915–922.
- VINCENT, A., LI, Z., HART, A., BARRETT-JOLLEY, R., YAMAMOTO, T., BURGESS, J., WRAY, D., BYRNE, N., MOLENAAR, P. & NEWSOME-DAVIS, J. (1993). Seronegative myasthenia gravis. Evidence for plasma factor(s) interfering with acetylcholine receptor function. *Annals of the New York Academy of Sciences* **681**, 529–538.
- WATTERS, D. & MAELICKE, A. (1983). On the organization of ligand binding sites at the acetylcholine receptor; a study with monoclonal antibodies. *Biochemistry* **22**, 1811–1819.

#### Acknowledgements

We thank M. Hammel for excellent technical assistance. This work was supported by the Deutsche Forschungsgemeinschaft (grant Fr-698/3-1).

Received 27 July 1995; accepted 25 October 1995.